

A Geochemical Classification for Feldspathic Igneous Rocks

B. RONALD FROST* AND CAROL D. FROST

DEPARTMENT OF GEOLOGY AND GEOPHYSICS, UNIVERSITY OF WYOMING, LARAMIE, WY 82072, USA

RECEIVED MAY 13, 2008; ACCEPTED OCTOBER 3, 2008
ADVANCE ACCESS PUBLICATION NOVEMBER 20, 2008

In this paper we classify the range of feldspathic igneous rocks using five geochemical variables: the $\text{FeO}/(\text{FeO} + \text{MgO})$ ratio or Fe-index, the modified alkali–lime index, the aluminum-saturation index, the alkalinity index, and the feldspathoid silica-saturation index. The Fe-index distinguishes between melts that have undergone extensive iron enrichment during differentiation from those that have not. The transition from tholeiite to ferrobasalt allows us to extend this boundary to silica values as low as 48 wt %. We introduce the feldspathoid silica-saturation index, which, coupled with the alkalinity index, allows us to extend the geochemical classification to alkaline rocks. We show that most alkaline rocks are ferroan and that this probably reflects extensive fractional crystallization of olivine and pyroxene with minimal participation of Fe–Ti oxides. The expanded classification allows us to illustrate the geochemical and petrogenetic relationship of the plutonic rocks from ferroan granites to nepheline syenites that commonly occur in intracratonic environments. It also allows us to distinguish four families of feldspathic rocks: (1) magnesian rocks, which are exemplified by Caledonian and Cordilleran batholiths and are characterized by differentiation under oxidizing and relatively hydrous conditions; (2) ferroan rocks, which include fayalite granites, alkali granites, and nepheline syenites and are characterized by differentiation under reducing and relatively dry conditions; (3) leucogranites, which commonly form by crustal melting; (4) potassic and ultrapotassic rocks, which originate from mantle that has been enriched in K_2O .

KEY WORDS: granite; rhyolite; geochemistry; classification; nepheline syenite; alkaline rocks; phonolite

INTRODUCTION

Several years ago we introduced a geochemical classification for granitic rocks (Frost *et al.*, 2001). In that scheme we suggested that granitic rocks could be classified using

three compositional variables, $\text{FeO}/(\text{FeO} + \text{MgO})$ (or Fe-index), $\text{Na}_2\text{O} + \text{K}_2\text{O} - \text{CaO}$ (or the modified alkali–lime index, MALI), and the aluminum-saturation index [ASI; molecular $\text{Al}/(\text{Ca} - 1.67\text{P} + \text{Na} + \text{K})$]. The scheme has achieved wide use but several issues remain unaddressed. One is whether the ferroan–magnesian boundary can be extended to intermediate and basic rocks. Another is the petrological significance of the alkalic, alkali–calcic, calc–alkalic and calcic boundaries in the MALI diagrams. In addition to addressing these questions, we extend our classification scheme by introducing two additional indices: the alkalinity index (AI) and feldspathoid silica-saturation index (FSSI). These indices allow for the discrimination of metaluminous from peralkaline rocks and silica-saturated from silica-undersaturated rocks, and thereby allow the geochemical classification scheme of Frost *et al.* (2001) to be extended to alkaline rocks. The enlarged classification scheme can be applied to the whole range of feldspathic rocks; that is, rocks in which feldspars (\pm quartz or feldspathoids) are the dominant minerals.

REVISIONS TO THE GEOCHEMICAL CLASSIFICATION OF GRANITES

Fe-index: the boundary between ferroan and magnesian rocks

The $\text{FeO}/(\text{FeO} + \text{MgO})$ ratio of rocks is an important indication of the fractionation history of a suite of rocks. If the rocks are reduced [FMQ (fayalite–magnetite–quartz) or below, Frost & Lindsley, 1992] fractional crystallization results in iron enrichment, whereas if the rocks are relatively oxidized (FMQ + 2 or more, Frost & Lindsley, 1992) the crystallization of magnetite inhibits iron

*Corresponding author. E-mail: rfrost@uwyo.edu

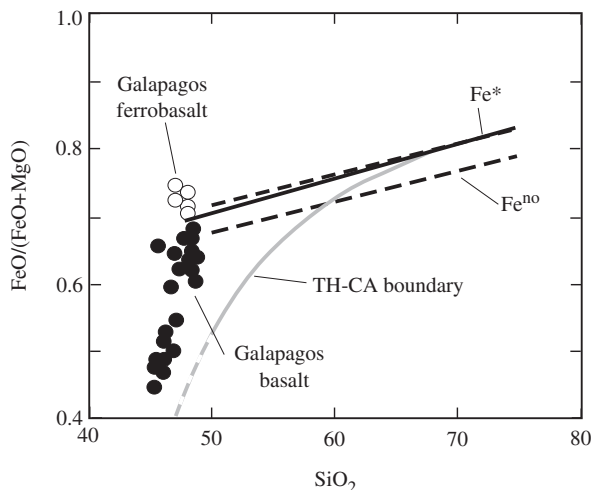


Fig. 1. Comparison of the ferroan–magnesian boundaries (Fe^* and Fe^{no}) of Frost *et al.* (2001; dashed lines) with the revised boundary proposed here (continuous line described by $\text{FeO}^*/(\text{FeO}^* + \text{MgO}) = 0.46 + 0.005\text{SiO}_2$) and the TH–CA boundary of Miyashiro (1974). Ferrobasalt–basalt transition from the Galapagos is after McBirney & Williams (1969). TH, ‘tholeiitic’; CA, ‘calc-alkalic’; $\text{Fe}^* = \text{FeO} + 0.9\text{Fe}_2\text{O}_3 / (\text{FeO} + 0.9\text{Fe}_2\text{O}_3 + \text{MgO})$; $\text{Fe}^{\text{no}} = \text{FeO} / (\text{FeO} + \text{MgO})$.

enrichment (Osborn, 1959). Miyashiro (1974) established a boundary between volcanic rocks that underwent an iron-enrichment trend and those that did not, which he identified as ‘tholeiitic’ and ‘calc-alkalic’ respectively. (Note: to eliminate confusion, we place the terms ‘tholeiitic’ and ‘calc-alkalic’ in quotation marks when they are applied *sensu lato* rather than *sensu stricto*.) Miyashiro’s boundary was determined from a suite of arc-related volcanic rocks from northeastern Japan, plotted on a diagram of FeO^*/MgO (where $\text{FeO}^* = \text{FeO} + 0.9\text{Fe}_2\text{O}_3$) against SiO_2 . He showed that the ‘calc-alkalic’ series could be separated from the ‘tholeiitic’ series by a straight line of the form $\text{FeO}^*/\text{MgO} = 0.157\text{SiO}_2 - 6.719$. This boundary, which is linear in a plot of FeO^*/MgO vs SiO_2 , is strongly curved in a plot of $\text{FeO}^*/(\text{FeO}^* + \text{MgO})$ vs SiO_2 (Fig. 1).

Frost *et al.* (2001) established their boundary between ferroan and magnesian granites as a straight line that separated a population of A-type granites from Cordilleran granites. They recognized two boundaries: Fe^{no} , which is the boundary determined from rocks in which both FeO and Fe_2O_3 have been analyzed, and Fe^* , which applies to rocks in which only the total amount of FeO (or Fe_2O_3) has been determined (Frost *et al.*, 2001; Fig. 1). Frost *et al.* (2001) drew their Fe^* boundary so that at high silica contents it coincided with the boundary of Miyashiro (1974). Because the boundary proposed by Miyashiro (1974) and that by Frost *et al.* (2001) diverge at $\text{SiO}_2 < 60\%$ the question arises which should be used for rocks with low silica.

The analyses that Frost *et al.* (2001) used to establish their boundary generally had $\text{SiO}_2 > 60.0\%$. To extend the ferroan–magnesian boundary to lower silica values we

plot ferrobasalts and basalts from the Galapagos, the type area where ferrobasalt was defined (McBirney & Williams, 1969). The ferrobasalt–basalt boundary from the Galapagos, which occurs in rocks with 48–50% SiO_2 , more than 13% total iron and less than 6% MgO , agrees remarkably well with the extrapolation of the Frost *et al.* (2001) boundary. Our revised boundary [calculated on the basis of total iron in the rock; $\text{FeO}^* = \text{FeO} + 0.9\text{Fe}_2\text{O}_3 / (\text{FeO} + 0.9\text{Fe}_2\text{O}_3 + \text{MgO})$] has a slightly steeper slope and fits the equation $\text{FeO}^* = 0.46 + 0.005\text{SiO}_2$. Because it is defined at low silica by the ferrobasalt–basalt transition, this boundary is applicable to rocks with silica as low as 48%.

The modified alkali–lime index (MALI)

Frost *et al.* (2001) defined the modified alkali–lime index from a plot of $\text{Na}_2\text{O} + \text{K}_2\text{O} - \text{CaO}$ vs SiO_2 . They plotted compositions from the Peninsular Ranges batholith, Tuolumne intrusive suite, the Sherman batholith, and Bjerkreim–Sokndal intrusion on this diagram and used them to draw boundaries between calcic, calc-alkalic, alkali–calcic, and alkalic series. Each boundary is constrained to go through MALI = 0 at the value defined by Peacock (1934) (namely, alkalic – alkali–calcic at $\text{SiO}_2 = 51.0$, alkali–calcic – calc-alkalic at $\text{SiO}_2 = 56.0$, and calc-alkalic – calcic at $\text{SiO}_2 = 61.0$). From these constraints, the boundaries were drawn by eye to separate as much as possible the individual suites. Below we discuss why the boundaries have the shape that they do and why mafic rocks commonly plot with trends that show large changes in MALI with small changes in silica.

MALI and igneous minerals

The first step to understand how MALI varies in rocks is to note where common igneous minerals plot on a MALI diagram (Fig. 2). The MALI value of plutonic rocks is the sum of the MALI values of the constituent minerals. The fractionation trend of a volcanic suite is controlled by the MALI of the mineral assemblages that are crystallized and extracted from the melt. As Fig. 2 shows, the minerals that contribute most to produce rocks with high MALI values are K-feldspar, albite, and nepheline (Fig. 2), whereas augite has the lowest MALI values. It is evident from Fig. 2 that, for rocks with more than about 60% SiO_2 , MALI is controlled by the abundances and compositions of feldspars and quartz, whereas at lower silica the extraction of augite during fractionation of more mafic rocks will have a powerful effect in increasing MALI in the residual magma.

Role of feldspars

To illustrate the role of feldspars in MALI we show a number of model rock compositions (Table 1) on a diagram of SiO_2 vs MALI (Fig. 3). The suite of model granitoids from diorite to trondjemite follows a trend roughly

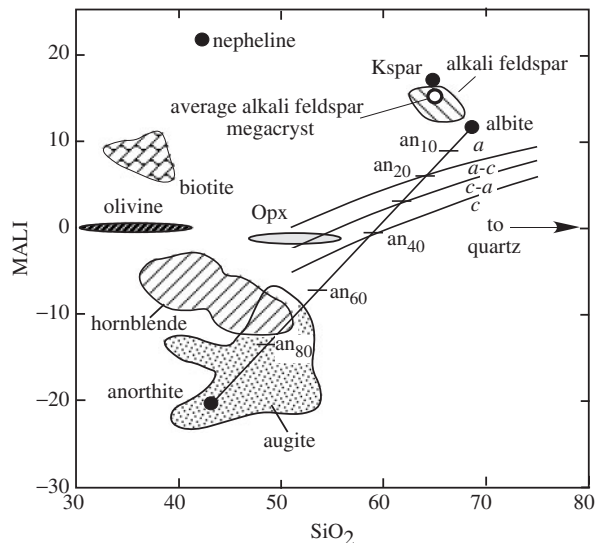


Fig. 2. The location of various igneous minerals on plot of MALI against SiO₂. a, alkalic; a-c, alkali-calcic; c-a, calc-alkalic; c, calcic; boundaries after Frost *et al.* (2001). Data from Deer *et al.* (1962, 1963) and Vernon (1986).

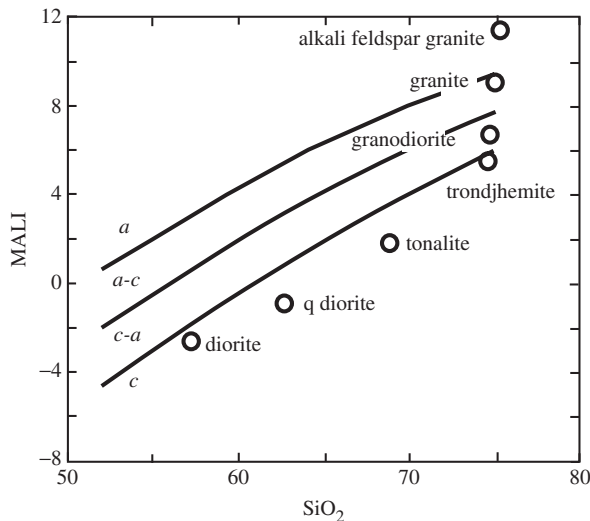


Fig. 3. MALI as a function of SiO₂, showing where the model granitoids listed in Table 1 plot. Abbreviations as in Fig. 2.

Table 1: Modes and compositions used for model rocks

Rock	% Plag	% Kspar	% Q
Diorite	100 (An ₄₅)	0	0
Quartz diorite	90 (An ₄₀)	0	10
Tonalite	80 (An ₃₀)	0	20
Trondjemite	70 (An ₂₀)	0	30
Granodiorite	45 (An ₂₀)	25	30
Granite	25 (An ₂₀)	45	30
Alkali feldspar granite	7 (An ₁₀)	63	30

parallel to the boundary between the calcic and calc-alkalic fields. In contrast, those granitoids that have increasing proportions of K-feldspar to plagioclase lie at progressively higher MALI values. Our simple calculations suggest that the shape of the boundaries in the MALI diagram reflects the increases in the abundance of Kspar and in the albite component of plagioclase with increasing silica in plutonic rocks. For volcanic suites, the trend reflects the changes in normative abundances of these two feldspar end-members.

To further emphasize the role of feldspars in the alkali-lime index we have plotted the modes of some of the suites that we used to define the MALI boundaries. Because modal mineralogy data are sparse for the Sherman batholith (Frost *et al.*, 1999) and Bjerkreim-Sokndal intrusion (Duchesne & Wilmart, 1997), our type alkali-calcic and alkalic granitoids, we have plotted instead data from the alkali-calcic Ballachulish (Weiss & Troll, 1989) and alkalic

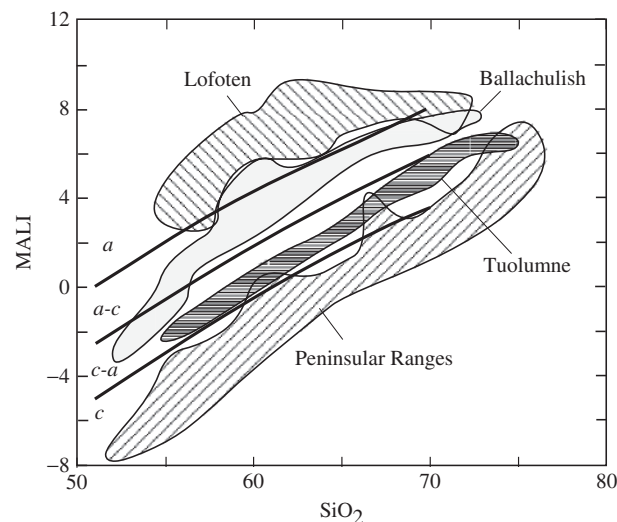


Fig. 4. Plot of MALI against SiO₂ showing the composition ranges of the Peninsular Ranges, Tuolumne, Ballachulish, and Lofoten batholiths. Abbreviations as in Fig. 2. Data from Larsen (1948), Malm & Ormaasen (1978), Bateman & Chappell (1979), and Weiss & Troll (1989).

Lofoten (Malm & Ormaasen, 1973) batholiths (Fig. 4). A plot of the modal data for the four plutons from Fig. 4 on a QAP diagram (Le Maitre, 1989; Fig. 5) illustrates how differences in the MALI reflect differences in the feldspar composition. The rocks of the Peninsular Ranges batholith, which is a calcic series, follow a trend from diorite to quartz diorite to tonalite to granodiorite. In contrast, the granitic rocks of Lofoten, an alkalic granitoid, follow the trend monzonite to quartz syenite to alkali feldspar granite (Fig. 5).

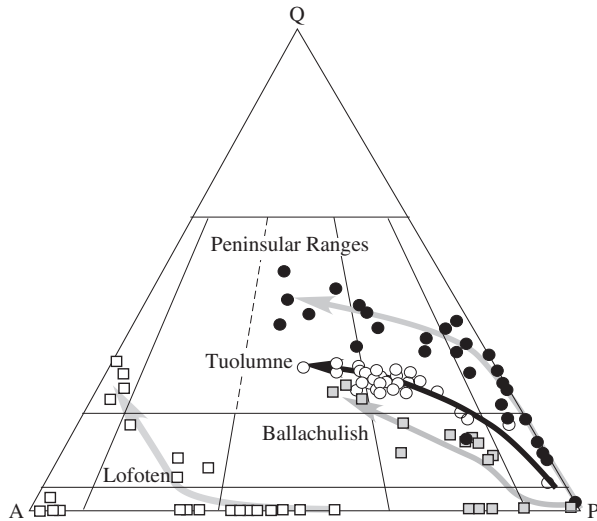


Fig. 5. QAP diagram showing the trends in modal mineralogy of rocks from the Peninsular Ranges, Tuolumne, Ballachulish, and Lofoten batholiths. Sources of data as in Fig. 4.

Our calculations indicate that fractional crystallization of feldspathic melts should lead to trends that lie parallel to the MALI boundaries we established earlier (Frost *et al.*, 2001). We have found, however, many igneous suites that cross these boundaries. We can postulate several causes for this. One is simple cumulate processes. Accumulation of K-feldspar and albite could drive the rock composition toward relatively high MALI values (Fig. 6a) and could cause magmas that are calcic or calc-alkalic to crystallize granitoids that are alkali-calcic or alkalic. Another process is mixing of magmas. An example of this is illustrated by the Sybille intrusion, a hot, dry ferroan granitoid that was emplaced into weakly peraluminous, calc-alkalic gneisses (Scoates *et al.*, 1996). The Sybille is strongly alkalic at low silica contents and becomes progressively more calcic as silica contents increase (Fig. 6b). This is probably caused by assimilation of small amounts of highly siliceous partial melts from the surrounding gneiss. Assimilation also drives the more siliceous rocks of the Sybille intrusion to more peraluminous compositions (Fig. 6c).

The aluminum-saturation index (ASI)

The third variable Frost *et al.* (2001) used in the classification of granites is the aluminum-saturation index (ASI), which was defined as molecular $Al / (Ca - 1.67P + Na + K)$ (Shand, 1947; Zen, 1988), which separates rocks into metaluminous and peraluminous varieties. Peraluminous varieties ($ASI > 1$) have more Al than is necessary to make feldspars. We noted (Frost *et al.*, 2001) that rocks with $ASI < 1$ are metaluminous when molecular $Na + K < Al$, and are peralkaline when molecular $Na + K > Al$. In this paper we introduce an additional classification diagram

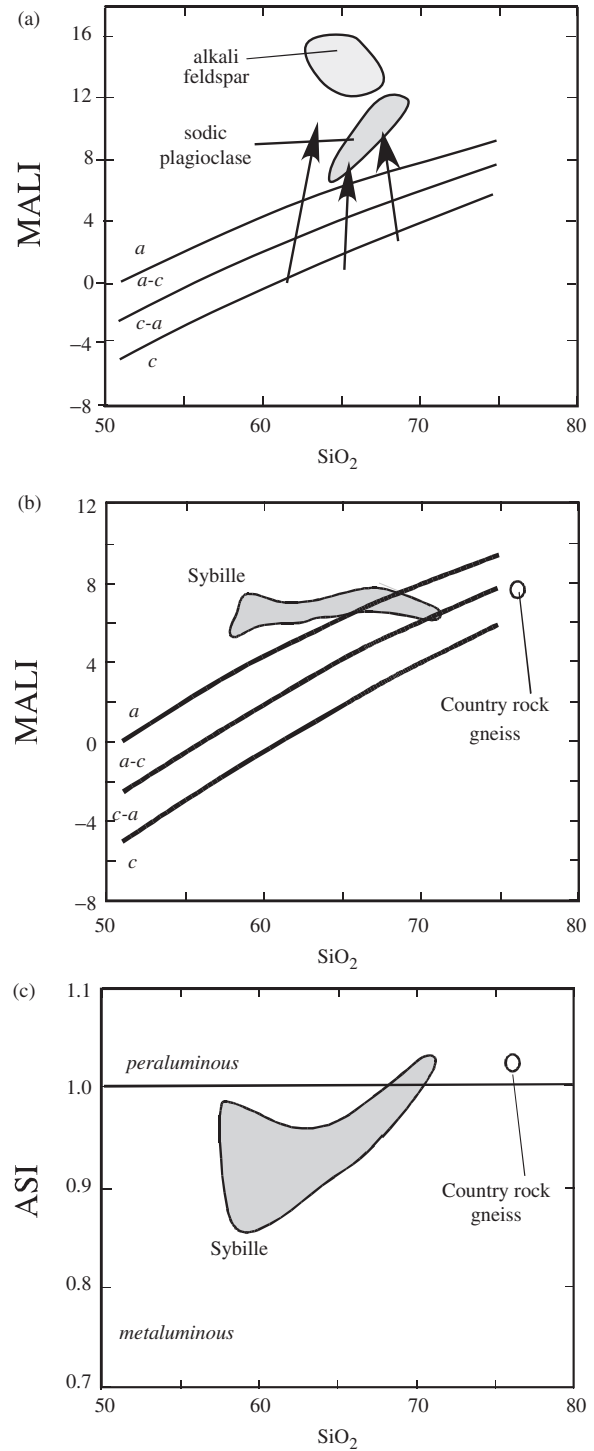


Fig. 6. Effects of feldspar accumulation and mixing on granitic composition indices. (a) MALI diagram showing how alkali feldspar accumulation (arrows) can drive a plutonic rock to compositions more alkalic than the magma from which it crystallized. (b) MALI diagram showing how the assimilation of calc-alkalic country-rock gneiss made the more silica-rich portions of the Sybille monzosyenite more calcic. (c) Plot of ASI vs silica showing how the assimilation of country-rock gneiss made the more silica-rich portions of the Sybille monzosyenite more aluminous (data from Scoates *et al.*, 1996).

that allows us to discriminate peralkaline rocks from metaluminous and peraluminous ones.

A GEOCHEMICAL CLASSIFICATION OF ALKALINE ROCKS

Alkaline rocks were not explicitly included in our original granite classification scheme (Frost *et al.*, 2001). However, some ferroan granites, such as the Sherman and Pikes Peak batholiths, contain units that are alkaline and many alkaline complexes contain both nepheline syenites and granites. Furthermore, there is ample evidence that ferroan granites, alkaline granites, and alkaline syenites form in similar intraplate, extensional environments. Therefore, it is useful to expand our geochemical scheme so that it includes both alkaline rocks and granitic rocks.

It is important to note that although the terms peralkaline, alkalic, and alkaline describe similar chemical characteristics they are not synonyms. As noted above, peralkaline rocks contain more alkalis than alumina on a molecular basis. Alkalic rocks are rocks that have high $\text{Na}_2\text{O} + \text{K}_2\text{O}$ relative to CaO as identified on a MALI diagram. These rocks can be metaluminous or peralkaline (or rarely peraluminous). Alkaline rocks were defined by Shand (1922) as rocks in which the molecular ratio of $\text{Na} + \text{K}$ to Al and Si is in excess of 1:1.6; that is, rocks for which either alumina or silica or both are deficient such that the rock contains higher alkalis than can be accommodated in feldspar alone. Alkaline rocks include both silica-saturated peralkaline rocks and silica-undersaturated rocks that may be either peralkaline or metaluminous.

The alkalinity and feldspathoid silica-saturation indices

The various types of alkaline rocks can be distinguished using two geochemical indices: the alkalinity index (AI) and the feldspathoid silica-saturation index (FSSI).

The alkalinity index (AI)

The alkalinity index (AI) is based on the definition by Shand (1947), and is defined as $\text{AI} = \text{Al} - (\text{K} + \text{Na})$ on a molecular basis. Peralkaline rocks have $\text{AI} < 0$, whereas metaluminous and peraluminous rocks have $\text{AI} > 0$. This index is often called agpaitic index. In its original usage, the term agpaitic was essentially synonymous with peralkaline (Ussing, 1912). However, the term agpaitic is now generally restricted to peralkaline nepheline syenites containing complex Zr and Ti minerals (Sørensen, 1960). Because we apply this index to rocks that can be either saturated or undersaturated in silica, we prefer to call this the alkalinity index.

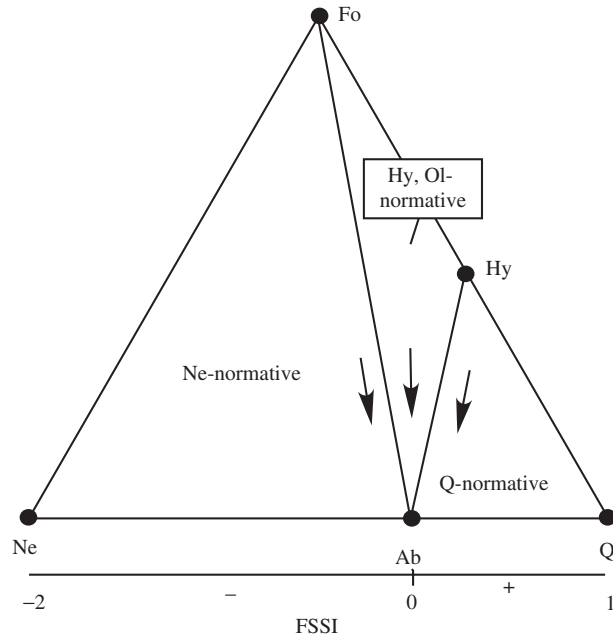


Fig. 7. Plot showing the nature of the feldspathoid silica-saturation index (FSSI). Arrows show the FSSI in the projection from within the Q–Ne–Fo triangle onto the Ne–Q plane.

The feldspathoid silica-saturation index (FSSI)

We need one more index to discriminate alkaline rocks that are silica-saturated from those that are silica-undersaturated. Because one cannot determine whether a rock is silica-saturated without calculating a norm, we define the feldspathoid silica-saturation index as normative $Q - [\text{Lc} + 2(\text{Ne} + \text{Kp})]/100$. In this index normative Ne and Kp are multiplied by two because each mole of nepheline or kaliophilite consumes 2 moles of quartz to make albite or orthoclase. When $\text{FSSI} > 0$ the rock is silica-saturated; when $\text{FSSI} < 0$ it indicates a rock is silica-undersaturated. This index collapses the basalt tetrahedron onto the quartz–nepheline line (Fig. 7). Rocks that plot in the Ne-normative field project to the Ne–Q line on a trajectory parallel to the Ol–Ab tie line; rocks with normative olivine and hypersthene but no normative Ne or Q project to $\text{FSSI} = 0$; and rocks in the Q-normative field project to the Ne–Q line on a trajectory parallel to the Hy–Ab tie line (Fig. 7). The projection represented by the FSSI is appropriate for our classification because we are dealing with feldspathic rocks where feldspars + feldspathoids or quartz are the most abundant minerals in the rock.

A plot of FSSI vs AI defines four quadrants (Fig. 8). Rocks with positive FSSI and AI plot in the upper right of this diagram and include metaluminous (or peraluminous) granites. The three remaining quadrants are occupied by alkaline rocks. Si-deficient alkaline rocks plot in the upper left. These are dominated by metaluminous alkaline rocks, although rare peraluminous alkaline rocks

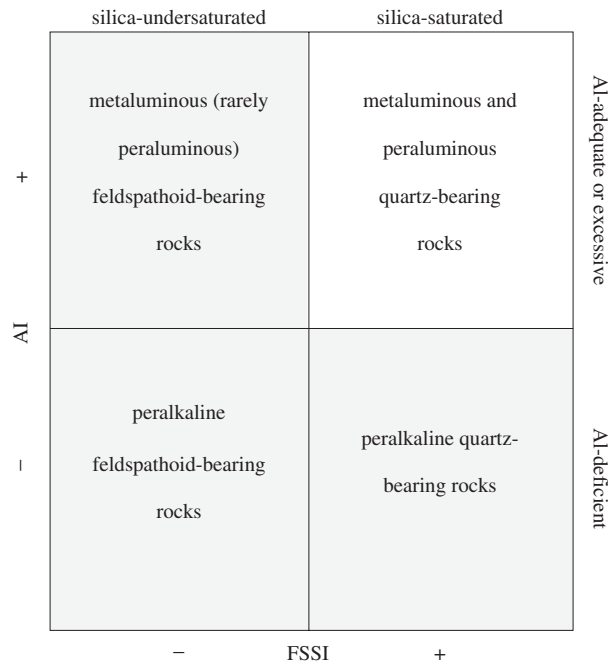


Fig. 8. Plot of alkalinity index (AI) vs feldspathoid silica-saturation index (FSSI) showing the fields for the various types of feldspathic rocks. Shaded fields represent alkaline rocks.

(e.g. Uppalapadu, Krishna Reddy *et al.*, 1998; Kumar *et al.*, 2007) also plot in this field. Si-saturated Al-deficient alkaline rocks plot in the lower right. These include peralkaline granite and its volcanic equivalents, pantellerite and comendite. Al- and Si-deficient alkaline rocks plot in the lower left quadrant, and include peralkaline nepheline syenite and its volcanic equivalent peralkaline phonolite.

DISCUSSION

The nature of alkaline igneous rocks

Fe-index

With few exceptions alkaline plutonic and volcanic rocks are ferroan (Fig. 9). Most suites, both plutonic (Fig. 9a and b) and volcanic (Fig. 9c and d), form bands that trend to increasing Fe^* with increasing silica. Many volcanic suites that are inferred to have formed mainly by fractional crystallization (e.g. Boina, Barberi *et al.*, 1975) show a continuous variation in silica; others, such as Pantelleria (Civetta *et al.*, 1998) are bimodal (Fig. 9c). The felsic portions of these suites may have formed by partial melting of the mafic rocks during later injections of mafic magma and heat into the system. It is virtually impossible to distinguish extreme differentiates of basalt from partial melts of basalt using major elements; therefore we include these bimodal suites with the differentiated suites. Volcanic suites that involve processes in addition to fractional crystallization tend to have a wider variation in Fe-index at any silica

value (Fig. 9d). One suite that shows no increase in Fe-index with increasing silica is the lamproites of the Leucite Hills (Fig. 9d), which have been interpreted to record different degrees of melting or derivation by melting of different assemblages in the mantle (Mirnejad & Bell, 2006).

MALI

Most suites of alkaline plutonic rocks are alkalic and at $SiO_2 < 60\%$ tend to have much steeper trends on MALI diagram than is typical of most metaluminous and peraluminous granites (Fig. 10a and b). Those suites with the lowest silica activity, such as Shonkin Sag or Nyambeni, tend to have the steepest slopes whereas those that are silica-saturated, such as Boina, tend to follow a slope close to that of the alkali-calcic – alkali boundary. This shallower slope reflects the effect of increasing abundance (either modal or normative) of quartz, which increases SiO_2 without changing MALI. At high MALI values, some Ne-bearing plutons (such as St. Hilaire and Ilimaussaq) tend to have slopes that decrease in silica with increasing MALI. This apparently is caused by increasing proportions of nepheline in the rocks.

Many volcanic suites that are proposed to have formed by fractional crystallization, such as Boina (Barberi *et al.*, 1975) and Nyambeni (Brotzu *et al.*, 1983) (Fig. 10c), form bands that show a continuous increase in MALI with increasing silica, although some suites are bimodal. Those that formed by other processes are not likely to show such a clear trend (Fig. 10d). A good example is the Leucite Hills lavas, which define three isolated fields.

AI and FSSI

Igneous suites typically have their highest AI when FSSI ~ 0 , with AI decreasing as FSSI either increases or decreases (Fig. 11). This is particularly well illustrated in Ne-bearing sodic volcanic suites that have formed by fractional crystallization and by Ne-bearing plutonic sites (Fig. 11a and c). The decrease in AI with increasing Fe^* for sodic suites indicates that AI tends to decrease as plagioclase crystallization enriches the residual magma in alkalis during differentiation (Fig. 12). In contrast, other plutonic suites tend to form irregular fields (Fig. 11b). Some of these suites cross from silica-undersaturated to silica-saturated with increased amounts of crustal assimilation (e.g. Red Hill; Henderson *et al.*, 1989). Volcanic suites that involve processes in addition to fractional crystallization (Fig. 11d) also tend to form irregular-shaped fields that show no obvious trend on an AI vs FSSI diagram. For example, Vesuvius magmas formed from mantle sources variably contaminated by slab-derived components, assimilated Hercynian crust, and Mesozoic limestone at mid-crustal depths (Di Renzo *et al.*, 2007). Incorporation of these various assimilants produces different trends on the classification diagrams.

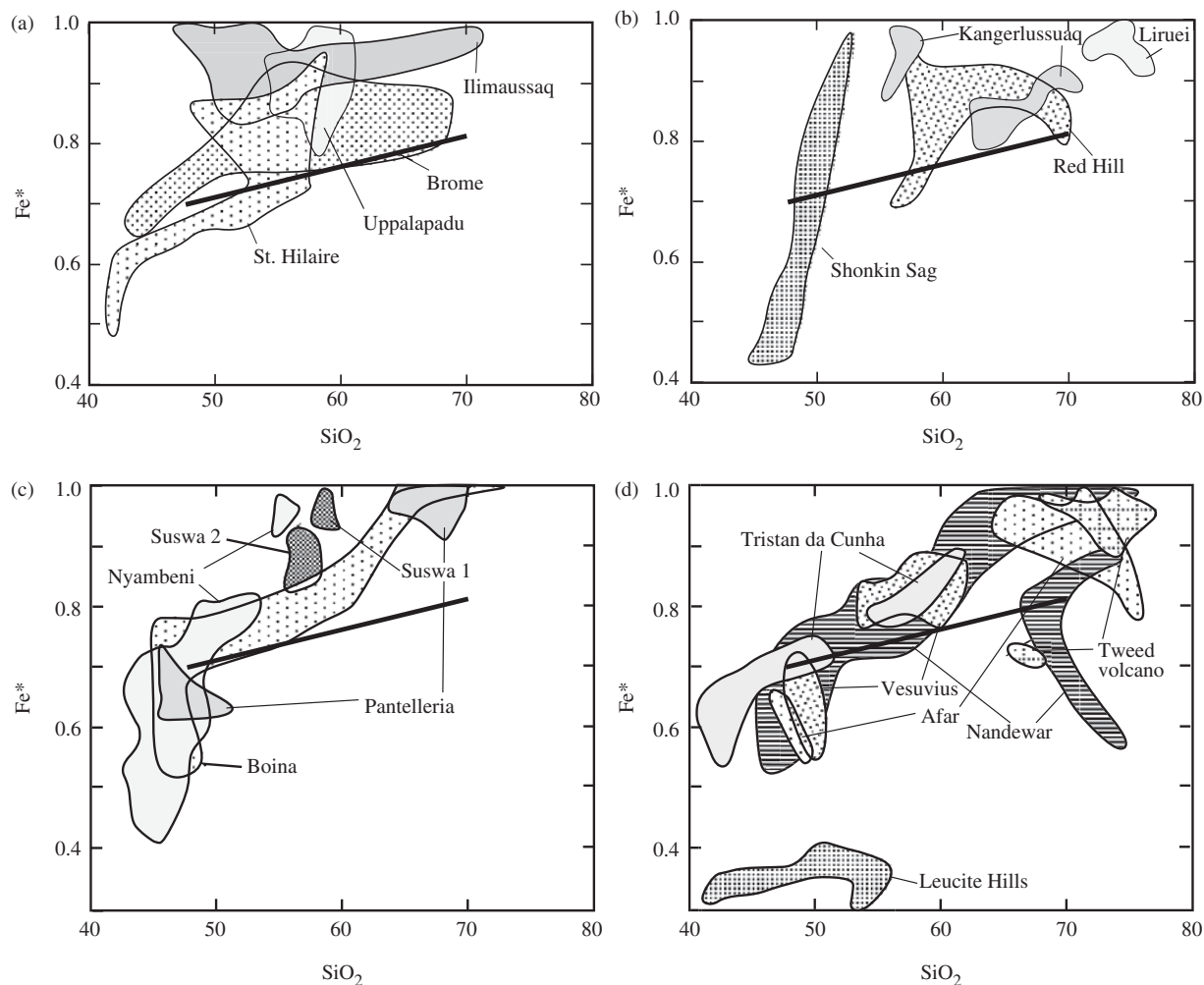


Fig. 9. Variation of Fe^* in alkaline rocks; boundary as in Fig. 1. (a) Nepheline-bearing plutonic rocks; (b) ultrapotassic alkaline plutonic rocks and plutonic suites, portions of which contain quartz; (c) volcanic rocks that formed by fractional crystallization; (d) volcanic rocks that evolved by processes other than (or in addition to) fractional crystallization. Ferroan–magnesian boundary as in Fig. 1. Data from Jacobson *et al.* (1958), Carmichael (1967), Abbott (1969), Nash *et al.* (1969), Ferguson (1970), Nash & Wilkinson (1970, 1971), Valiquette & Archambault (1970), Barberi *et al.* (1974, 1975), Ewart *et al.* (1977), Brotzu *et al.* (1983), Eby (1985), Stoltz (1985), Currie *et al.* (1986), Orajaka (1986), Czygan & Goldenberg (1989), Henderson *et al.* (1989), Le Roex *et al.* (1990), Civetta *et al.* (1998), Krishna Reddy *et al.* (1998), Bailey *et al.* (2001), Mirnejad & Bell (2006), Di Renzo *et al.* (2007), Kumar *et al.* (2007) and Riishuus *et al.* (2008).

The trends shown in Fig. 11 reflect two processes that accompany differentiation of igneous rocks, as follows.

(1) Melts generally evolve away from the thermal divide ($AI = 0.0$) towards minima (and under some conditions eutectics) involving either feldspars + feldspathoids or feldspars + quartz. Extraction of low-silica phases such as olivine and hornblende enriches a hypersthene-normative melt in silica, whereas crystallization of high-silica phases such as aegirine and feldspars drives nepheline-normative melts away from the silica saturation boundary. Fractional crystallization of low-silica phases such as Fe–Ti oxides and Na-amphiboles can cause some alkali basalts to evolve to silica-saturated rhyolites (e.g. Red Hill, Henderson *et al.*, 1989; Pantelleria, Civetta *et al.*, 1998). Crustal assimilation may cause the transition of magmas from undersaturated

($FSSI < 0$) to silica-saturated ($FSSI > 0$) as in the Kangerlussuaq intrusion (Riishuus *et al.*, 2008), but there is no known closed-system process that could drive saturated melts into the undersaturated field.

(2) There is a tendency for fractional crystallization of plagioclase and alkali feldspar to enrich the melt in sodium while depleting it in alumina. As a result, many of the suites cross from metaluminous to peralkaline with increasing differentiation. In Fig. 11c we plot the location of plagioclase of various compositions. Fractional crystallization of calcium-bearing plagioclase (with An as low as An₄₀) extracts alumina in preference to Na, thus decreasing the AI of the magma. This phenomenon, known as the ‘plagioclase effect’ (Bowen, 1945), can cause a primary melt in which molecular Ca is greater than Al to evolve toward

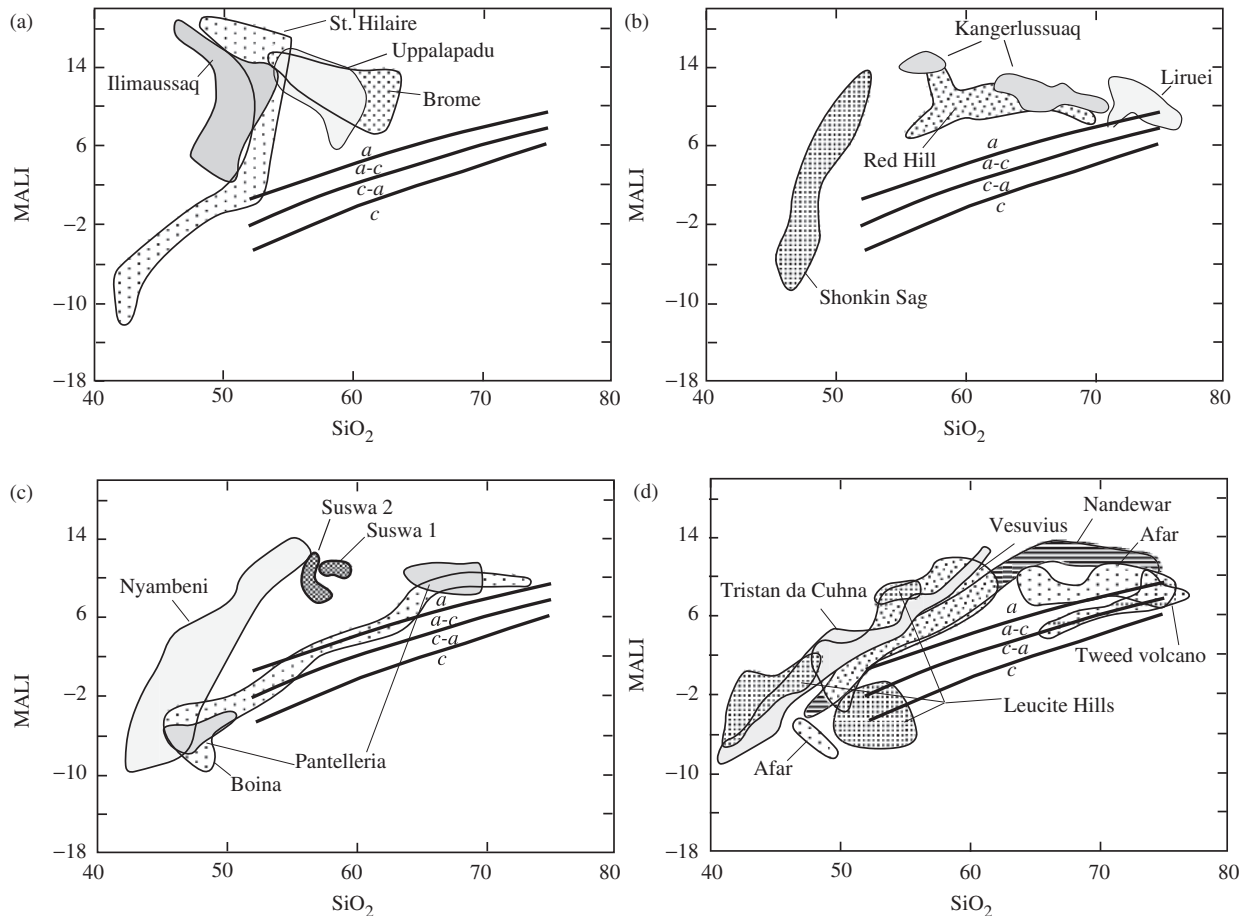


Fig. 10. Variations of MALI vs SiO_2 (wt %) in alkaline rocks. (a) Nepheline-bearing plutonic rocks; (b) ultrapotassic alkaline plutonic rocks and plutonic suites, portions of which contain quartz; (c) volcanic rocks that formed by fractional crystallization; (d) volcanic rocks that evolved by processes other than (or in addition to) fractional crystallization. Abbreviations as in Fig. 2; sources of data as in Fig. 9.

alkaline differentiates. For some suites (such as Nyabeni and Boina) the transition to peralkaline compositions is simply a manifestation of the plagioclase effect (Barberi *et al.*, 1975; Brotzu *et al.*, 1983). In addition to the plagioclase effect, alkaline rocks commonly evolve Na-rich fluids and addition of such fluids can increase the alkalinity of magmas (Bailey, 1974). Such a process has been postulated for the volcanic centers marginal to the Afar rift (Barberi *et al.*, 1974) and in the peralkaline nepheline syenites of Ilimaussaq (Schoenenberger *et al.*, 2006).

A classification of feldspathic rocks

Frost *et al.* (2001) based their granitoid classification on three indices: Fe-index, MALI and ASI. In this paper we have introduced the alkalinity index (AI) and the feldspathoid silica-saturation index (FSSI). These additional indices extend the original classification to encompass alkaline rocks. As is evident from Fig. 8, the AI and FSSI indices divide feldspathic rocks into four broad categories of plutonic rocks (and their volcanic equivalents): (1) metaluminous and peraluminous granitoids; (2) peralkaline

granitoids; (3) metaluminous feldspathoid-bearing syenites; (4) peralkaline feldspathoid-bearing syenites (Table 2).

Frost *et al.* (2001, table 1) categorized the varieties of granitoids on the basis of the Fe-index, MALI, and ASI. The alkaline rocks fall into the alkalic (or rarely alkali-calcic) peralkaline category in that table. With the addition of the AI and FSSI indices, we can expand the classification of alkaline rocks. This expanded classification is presented in Table 2, where the peralkaline granites are included along with other alkaline rocks. Of all the alkaline rock suites that we compiled, only Shonkin Sag, the phonotephrites of Vesuvius, and Leucite Hills are magnesian; all the others are ferroan.

Nature of intraplate magmatism

The fact that nearly all alkaline rocks are ferroan suggests that they most probably formed through extreme differentiation or partial melting of tholeiitic to alkalic mafic magmas, similar to other ferroan granites (Loiselle & Wones, 1979; Frost & Frost, 1997). It has long been

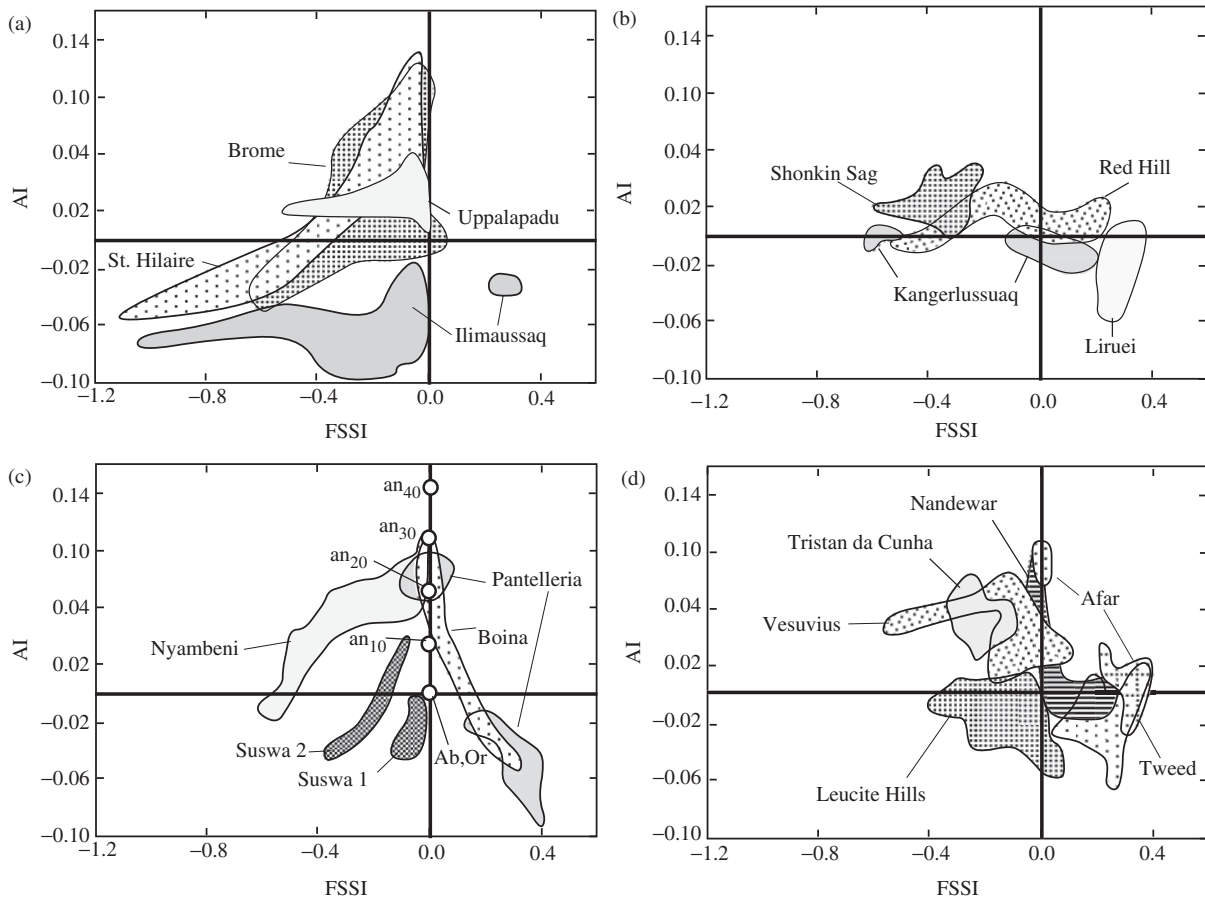


Fig. 11. FSSI vs AI plots for alkaline rocks. (a) Nepheline-bearing plutonic rocks; (b) ultrapotassic alkaline plutonic rocks and plutonic suites, portions of which contain quartz; (c) volcanic rocks that formed by fractional crystallization; (d) volcanic rocks that evolved by processes other than (or in addition to) fractional crystallization. Sources of data as in Fig. 9.

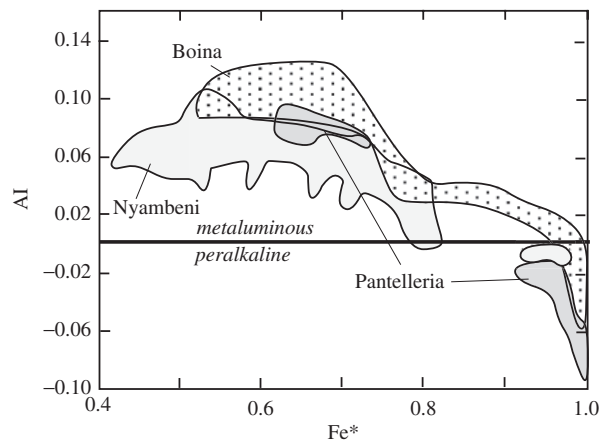


Fig. 12. Plot of AI vs Fe^* for volcanic rocks formed by fractional crystallization. Data from Barberi *et al.* (1975), Brotzu *et al.* (1983) and Civetta *et al.* (1998).

recognized that basaltic magmatism ranging from strongly Q-normative tholeiites to Ne-normative basanites is common in intracratonic rifts (Anthony *et al.*, 1992), although most rifts contain only a portion of this

compositional spectrum. Extreme fractional crystallization or partial melting of these melts leads to fayalite rhyolites (e.g. Snake River Plain and Yellowstone; Hildreth *et al.*, 1991; Hanan *et al.*, 2008; Whitaker *et al.*, 2008), peralkaline rhyolites (e.g. Boina; Barbari *et al.*, 1975), or peralkaline phonolites (e.g. Nyambeni; Brotzu *et al.*, 1983). The plutonic rocks equivalent to these volcanic rocks—fayalite granite, peralkaline granite, and peralkaline nepheline syenite—probably formed by the same processes (Fig. 13).

Emplacement and differentiation of tholeiitic magmas within the middle and upper crust produces layered mafic intrusions, the tops of which commonly contain ferroan syenites or granophyres (Fig. 13; Morse, 1980; Parsons, 1981). Emplacement and differentiation of similar magmas at the base of the crust leads to olivine, augite, and plagioclase cumulates (Emslie, 1985; Longhi & Ashwal, 1985). Plagioclase in these cumulates typically is sodic and considerably less dense than the surrounding magma or crust and could be emplaced diapirically to shallow crustal levels (Scoates, 2000). In addition, because the primary crystallization field for augite expands with increasing P ,

Table 2: Classification scheme for feldspathic rocks

Field	Peralkaline Si-saturated	Metaluminous Si-undersaturated	Peralkaline Si-undersaturated
<i>Plutonic rocks</i>			
Ferroan	Liruei (Jacobson <i>et al.</i> , 1958; Orajaka, 1986)	Uppalapadu (Czygan & Goldenberg, 1989; Krishna Reddy <i>et al.</i> , 1998; Kumar <i>et al.</i> , 2007)	Ilimaussaq (Ferguson, 1970; Bailey <i>et al.</i> , 2001)
Magnesian	None known	Lower portion of the Shonkin Sag (Nash & Wilkinson, 1970)	None known
<i>Volcanic rocks</i>			
Ferroan	Pantelleria (Civetta <i>et al.</i> , 1998)	Nyambeni (Brotzu <i>et al.</i> , 1983)	Evolved magmas of Suswa (Nash <i>et al.</i> , 1969)
Magnesian	None known	Phonotephrites from Vesuvius (Di Renzo <i>et al.</i> , 2007)	Leucite Hills (Carmichael, 1967; Mirnejad & Bell, 2006)

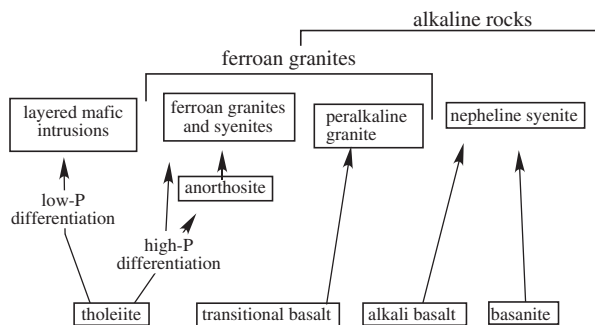


Fig. 13. Schematic diagram showing the relationships between intraplate feldspathic rocks and their inferred parental basalts.

the melt in equilibrium with Plag–Ol–Cpx will be aluminous and when it is emplaced into shallow levels it would lie in the primary crystallization field for plagioclase (Longhi *et al.*, 1993). Both these processes could lead to the formation of massif anorthosites (Fig. 13).

The residual magmas from anorthosites or from high-*P* differentiation of tholeiitic magmas may form potassic ferroan granites (Anderson *et al.*, 2003; Whitaker *et al.*, 2008). Extreme fractional crystallization or partial melting of basalts that are transitional between tholeiite and alkali basalt could lead to the formation of peralkaline granites (Barberi *et al.*, 1975; Loiselle & Wones, 1979), although peralkaline granites may also form by assimilation of siliceous crust by phonolitic magmas (e.g. Kangerlussuaq; Riishuus *et al.*, 2008). Finally, differentiation of alkali basalts and basanites will lead to the formation of nepheline syenites (Fig. 13). These syenites are likely to be metaluminous, unless the original magma had rather low abundances of normative An, in which case the plagioclase effect could cause these nepheline syenites to be peralkaline (Bowen, 1945).

Application to mafic rocks

Although in this paper we have plotted suites of rocks that contain samples with silica contents as low as 40%, our classification scheme does not distinguish well various types of basaltic rocks: basanite, alkali basalt, oceanic tholeiites, mid-ocean ridge basalts (MORB), and arc basalts all plot in the same area on MALI diagrams (Fig. 14a). Therefore, although MALI diagrams may depict the evolution of alkalis in mafic rocks, we suggest that the alkalic – alkali – calcic – calc-alkalic – calcic boundaries on the MALI diagrams are not usefully applied to rocks that have silica contents lower than 52%. We have chosen this silica value for two reasons. First, it marks the boundary between intermediate and mafic rocks (Le Maitre, 1989) and is a logical place to make a break. Second, the MALI diagram distinguishes suites of rocks dominated by feldspars (or feldspathoids) and mafic rocks are dominated instead by pyroxenes or amphiboles.

Because we have defined the Fe-index using ferrobasalts, this index can be used for rock suites with silica values as low as 48% (Fig. 14b). As noted above, it is helpful in distinguishing those suites that have undergone extensive differentiation under low oxygen fugacities from those that have not. The ferroan–magnesian boundary as we have defined it is fundamentally different from that of Miyashiro (1974). Our boundary distinguishes rocks that have undergone extensive iron enrichment from those that have not, whereas Miyashiro's boundary distinguishes suites that have undergone even moderate amounts of Fe enrichment (his 'tholeiitic' trend) from those that have undergone some Si enrichment (his 'calc-alkalic' trend). It is important to note that, at low silica, his boundary does not distinguish between tholeiitic and calc-alkalic rocks *sensu stricto*: for example, basalts from Giant Crater,

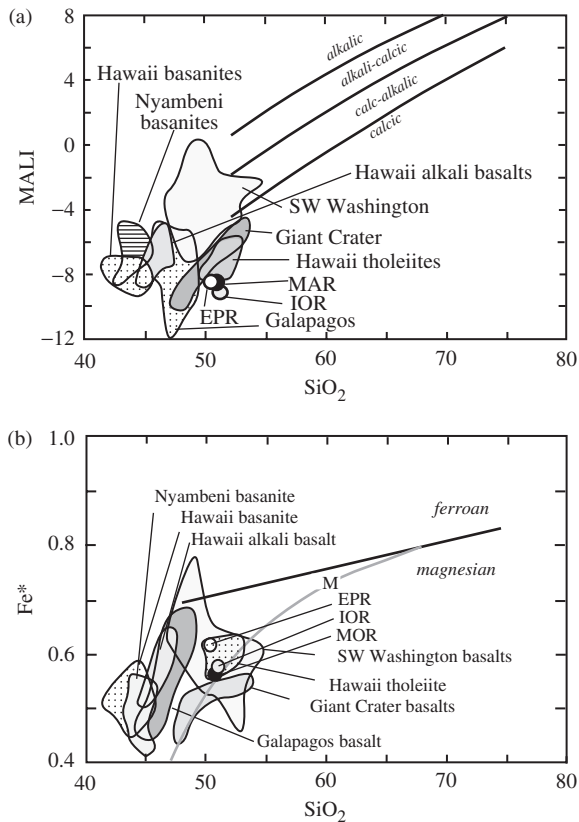


Fig. 14. Plots of SiO₂ vs (a) MALI and (b) Fe* for basaltic rocks. Data from MacDonald (1968), McBirney & Williams (1969), Brotzu *et al.* (1983), Leeman *et al.* (1990) and Baker *et al.* (1991). Average MORB from East Pacific Rise (EPR), Mid-Atlantic Ridge (MAR), and Indian Ocean Ridge (IOR) from Melson *et al.* (1976).

California, which bridge the boundary, are tholeiitic (i.e. Hy-normative) and calcic (not calc-alkalic) (Fig. 14) (Baker *et al.*, 1991).

Four families of feldspathic rocks

Our new classification scheme, when added to that of Frost *et al.* (2001), establishes that feldspathic igneous rocks fit into four broad families (Table 3). In order of relative abundance they are (1) magnesian rocks, (2) ferroan rocks, (3) leucogranites and (4) potassic and ultrapotassic rocks.

Magnesian

The magnesian rocks form granitoids that range in composition from tonalite through granodiorite to granite (and their volcanic equivalents). They range in composition from calcic to alkali-calcic (rarely alkalic) and may be either metaluminous or peraluminous. These rocks typically form in arcs and ‘post-collisional’ environments, and they obtain their magnesian signature because they undergo differentiation under oxidizing (and probably wet) conditions (Osborn, 1959). In addition, because much of the continental crust is composed of these magnesian granitoids, magmas derived by partial melting of continental crust may inherit this magnesian character.

Ferroan

The ferroan rocks range from fayalite granite (or rhyolite), through alkali granite (or pantellerite) to nepheline syenite (or phonolite). They are mostly alkalic, although some are alkali-calcic (Sherman batholith; Frost *et al.*, 1999) or even calc-alkalic (Lachlan; Collins *et al.*, 1982; King *et al.*, 2001). Most ferroan rocks are metaluminous or peralkaline,

Table 3: A classification scheme for feldspathic igneous rocks

Rock group	Characteristics	Rock types	Occurrence	Examples	References
Magnesian	Rocks that follow a relatively oxidizing differentiation trend with minor Fe enrichment	Tonalites, granodiorites, granites and their volcanic equivalents	Arc or post-collisional magmas or melts derived from earlier arc magmas	Tuolumne Etive	(Bateman & Chappell, 1979) (Frost & O’Nions, 1985)
Ferroan	Fe-rich rocks that have undergone extensive fractionation at low oxygen fugacity	Ferroan granites, alkali granites, nepheline syenites and volcanic equivalents	Evolved magmas from intraplate environments	Bjerkreim-Sokndal Ilimaussaq	(Duchesne & Wilmart, 1997) (Ferguson, 1970)
Leucogranite	High-silica granitoids that are commonly peraluminous	Peraluminous and metaluminous leucogranite	Crustal melts found in compressional tectonic environments	Manaslu Tetons	(La Fort, 1981) (Frost <i>et al.</i> , 2006)
Potassic	K-rich and ultra-K-rich mafic and felsic magmas	Lamproites and high-K shoshonites, phonotephrites	Rare, found in both intraplate and arc settings	Leucite Hills Roman Province	(Carmichael, 1967; Mirnejad & Bell, 2006) (Avanzinelli <i>et al.</i> , 2008)

although a few are peraluminous (Collins *et al.*, 1982; King *et al.*, 2001). They form in intraplate settings, mostly on continents, although evolved magmas from ocean islands also fall into this group (Haapala *et al.*, 2005; Bonin, 2007). The most Fe-rich of these rocks form by differentiation or partial melting of basaltic parents (Loiselle & Wones, 1979; Frost & Frost, 1997).

Leucogranites

Substantial volumes of leucogranites (or high-Si rhyolites) may form by differentiation (i.e. extraction of melt from “mush zones” in silicic magma chambers) Bachmann & Bergantz (2004). However, melting of crustal rocks with compositions ranging from metapelitic schist to metabasite may also produce leucogranites, most of which are peraluminous (Beard & Lofgren, 1991; Rapp *et al.*, 1991; Patino Douce & Beard, 1995, 1996). Pelitic and psammitic rocks melt to give leucogranites that range from ferroan to magnesian and from alkalic to calcic. Wet melting tends to make the melts rather calcic, because plagioclase is involved in the melting, whereas dehydration melting tends to make melts more alkalic because only micas are involved in these melting (Patiño Douce & Beard, 1996). Mafic rocks melt to give mostly magnesian, calcic melts. Most of these melts are peraluminous, although the ASI decreases with increasing pressure and temperature of melting (Rapp *et al.*, 1991). As expected, silica contents decrease with increasing temperature (i.e. increasing degree of melting) so that melts produced at the highest T (higher than *c.* 1000°C) are not true leucogranites.

Leucogranites produced by crustal melting probably make up important constituents of many batholiths. They are thought to be a major component of many tonalites (Beard, 1998; Smithies *et al.*, 2003). However, pure crustal melts are preserved in only a few environments. The most obvious environment is in Himalayan-type granites, which form through decompression melting. Because the formation of these leucogranites does not involve mafic magma as a heat source, melts produced by this process do not hybridize with more mafic magmas and are compositionally distinct. This is the type of granite identified by Frost *et al.* (2001) as peraluminous leucogranite.

Potassic and ultrapotassic rocks

The only feldspathic magnesian alkaline suites we have identified are potassic. Although arc magmas generated at increasingly greater depths generally become more potassic (Marsh & Carmichael, 1974), many potassic alkaline rocks are probably generated from melting of a mantle that has been enriched in a K-rich phase such as phlogopite, K-pargasite or K-hollandite (Conceição & Green, 2004; Mirnejad & Bell, 2006). They occur both in arc settings (e.g. Roman province; Avanzinelli *et al.*, 2008) and intraplate settings (e.g. Leucite Hills; Mirnejad & Bell, 2006). Unlike sodic rocks, where substantial plagioclase

crystallization is required to enrich the melt in alkalis (Bowen, 1945), potassic rocks emerge from the mantle already enriched in alkalis, hence their magnesian nature.

Summary

Although distinctive examples exist for all these families (Table 3), there are many examples of igneous suites that are gradational between these families. Silica-rich portions of Cordilleran batholiths share geochemical characteristics with leucogranites: at silica contents above 75%, Cordilleran batholiths tend to be peraluminous and have compositions that range from calcic to alkalic and from magnesian to ferroan, compositional ranges characteristic of leucogranites (Frost *et al.*, 2001, fig. 4). Peraluminous, leucocratic portions of ferroan batholiths also may be produced by crustal contamination. The late leucogranites associated with the Sherman batholith were formed by this means (Frost *et al.*, 1999).

Some convergent-margin magmas are transitional between magnesian and ferroan. For example, some transitionally ferroan Cordilleran intrusions, such as the Ironside Mountain batholith, have formed in areas of local extension within an overall convergent setting by fractional crystallization of a reduced, H₂O-poor tholeiite (Barnes *et al.*, 2006). Another example is the Taupo volcanic field of New Zealand, in which a suite of magnesian andesites to ferroan rhyolites occur in a rift along the Hikurangi subduction margin (Sutton *et al.*, 2000; Nicol & Wallace, 2007).

CONCLUSIONS

In this paper we have classified the whole range of feldspathic igneous rocks using five geochemical variables: the FeO/(FeO + MgO) ratio (Fe-index), the modified alkali-lime index (MALI), the aluminum-saturation index (ASI), the alkalinity index (AI), and the feldspathoid silica-saturation index (FSSI). The Fe-index can be used to determine whether feldspathic rocks undergo iron enrichment during differentiation, whereas the modified alkali-lime index reflects the compositions and abundances of feldspars in rocks. By introducing the feldspathoid silica-saturation index coupled with the alkalinity index we extend the geochemical classification to alkaline feldspathic rocks.

The classification scheme shows that most alkaline rocks are ferroan and are therefore relatives of ferroan granite (and ferroan rhyolite). Most members of this broad family of ferroan rocks obtained their geochemical signature by extreme differentiation or partial melting of basaltic rocks. Our classification scheme recognizes three other families of feldspathic rocks. The magnesian rocks are granitoids that have evolved under oxidizing conditions and that show only minor iron enrichment. Many leucogranites formed mainly by melting crustal rocks, and the

potassic family includes magmas typically produced in small volumes by partial melting of potassium-enriched mantle.

ACKNOWLEDGEMENTS

The authors would like to thank Gregor Markl, James S. Beard, Tapani Rämö, and an anonymous reviewer for helpful suggestions that improved the presentation of this paper.

REFERENCES

- Abbott, M. J. (1969). Petrology of Nandewar volcano, N.S.W., Australia. *Contributions to Mineralogy and Petrology* **20**, 115–134.
- Anderson, I. C., Frost, C. D. & Frost, B. R. (2003). Petrogenesis of the Red Mountain pluton, Laramie anorthosite complex, Wyoming: implications for the origin of A-type granites. *Precambrian Research* **124**, 243–267.
- Anthony, E. Y., Hoffer, J. M., Waggoner, W. K. & Chen, W. (1992). Compositional diversity in late Cenozoic mafic lavas in the Rio Grande rift and Basin and Range Province, southern New Mexico. *Geological Society of America Bulletin* **104**, 973–979.
- Avanzinelli, R., Elliott, T., Tommasini, S. & Conticelli, S. (2008). Constraints on the genesis of potassium-rich Italian volcanic rocks from U/Th disequilibrium. *Journal of Petrology* **49**, 195–224.
- Bachmann, O. & Bergantz, G. (2004). The origin of crystal-poor rhyolites: extracted from crystal-poor batholithic mushes. *Journal of Petrology* **45**, 1565–1585.
- Bailey, D. K. (1974). Experimental petrology relating to oversaturated peralkaline volcanics: A review. *Bulletin Volcanologique* **38**, 637–652.
- Bailey, J. C., Gwozdz, R., Rose-Hansen, J. & Sorensen, H. (2001). Geochemical overview of the Ilimaussaq alkaline complex, South Greenland. *Geology of Greenland Survey Bulletin, Report 190* **301**, 35–53.
- Baker, M. B., Grove, T. L., Kinzler, R. J., Donnelly-Nolan, J. M. & Wandless, G. A. (1991). Origin of compositional zonation (high-alumina basalt to basaltic andesite) in the Giant Crater Lava Field, Medicine Lake Volcano, Northern California. *Journal of Geophysical Research* **96**, 21819–21842.
- Barberi, F., Santacroce, R. & Varet, J. (1974). Silicic peralkaline volcanic rocks of the Afar Depression (Ethiopia). *Bulletin Volcanologique* **38**, 755–790.
- Barberi, F., Ferrara, G., Santacroce, R., Treuil, M. & Varet, J. (1975). A transitional basalt–pantellerite sequence of fractional crystallization, the Boina centre (Afar Rift, Ethiopia). *Journal of Petrology* **16**, 22–56.
- Barnes, C. G., Mars, E. V., Swapp, S. & Frost, C. D. (2006). Petrology and geochemistry of the Middle Jurassic Ironside Mountain batholith: evolution of potassic magmas in a primitive arc setting. In: Snoke, A. W. & Barnes, C. G. (eds) *Geological Studies in the Klamath Mountains Province, California and Oregon: a volume in honor of William P. Irwin* **410**, 199–221.
- Bateman, P. C. & Chappell, B. W. (1979). Crystallization, fractionation and solidification of the Tuolumne intrusive series, Yosemite National Park, California. *Geological Society of America Bulletin* **72**, 427–435.
- Beard, J. S. (1998). Polygenetic tonalite–trondjemite–granodiorite (TTG) magmatism in the Smartville Complex, Northern California with a note on LILE depletions in plagiogranites. *Mineralogy and Petrology* **64**, 15–45.
- Beard, J. S. & Lofgren, G. E. (1991). Dehydration melting and water-saturated melting of basaltic and andesitic greenstones and amphibolites at 1, 3, and 6–9 kb. *Journal of Petrology* **32**, 365–401.
- Bonin, B. (2007). A-type granites and related rocks: evolution of a concept, problems and prospects. *Lithos* **97**, 1–29.
- Bowen, N. L. (1945). Phase equilibria bearing on the origin and differentiation of alkaline rocks. *American Journal of Science* **243A**, 75–89.
- Brotzu, P., Morbidelli, L. & Piccirillo, E. M. (1983). The basanite to peralkaline phonolite suite of the Plio-Quaternary Nyambeni multicenter volcanic range (East Kenya Plateau). *Neues Jahrbuch für Mineralogie, Abhandlungen* **147**, 253–280.
- Carmichael, I. S. E. (1967). The mineralogy and petrology of the volcanic rocks from the Leucite Hills, Wyoming. *Contributions to Mineralogy and Petrology* **15**, 24–66.
- Civetta, L., D'Antonio, M., Orsi, G. & Tilton, G. R. (1998). The geochemistry of volcanic rocks from Pantelleria Island, Sicily Channel: petrogenesis and characteristics of the mantle source region. *Journal of Petrology* **39**, 1453–1491.
- Collins, W. J., Beams, S. D., White, A. J. R. & Chappell, B. W. (1982). Nature and origin of A-type granites with particular reference to southeastern Australia. *Contributions to Mineralogy and Petrology* **80**, 189–200.
- Conceição, R. V. & Green, D. H. (2004). Derivation of potassic (shoshonitic) magmas by decompression melting of phlogopite + pargasite lherzolite. *Lithos* **72**, 209–229.
- Currie, K. L., Eby, G. N. & Gittins, J. (1986). Petrology of the Mont Saint Hilaire complex, southern Quebec: an alkaline gabbro–peralkaline syenite association. *Lithos* **19**, 65–81.
- Czygan, W. & Goldenberg, G. (1989). Petrography and geochemistry of the alkaline complexes of Sivamalai, Elchuru and Uppalapadu, India. *Geological Society of India, Memoir* **15**, 225–240.
- Deer, W. A., Howie, R. A. & Zussman, J. (1962). *Rock-Forming Minerals. Vol. 3. Sheet Silicates*. Harlow: Longman.
- Deer, W. A., Howie, R. A. & Zussman, J. (1963). *Rock-Forming Minerals. Vol. 2. Chain Silicates*. Harlow: Longman.
- Di Renzo, V., Di Vito, M. A., Arienzo, I., Carandente, A., Civetta, L., D'Antonio, M., Giordano, F., Orsi, G. & Tonarini, S. (2007). Magmatic history of Somma Vesuvius on the basis of new geochemical and isotopic data from a deep borehole (Camaldoli della Torre). *Journal of Petrology* **48**, 753–784.
- Duchesne, J. & Wilmart, E. (1997). Igneous charnockites and related rocks from the Bjerkreim–Sokndal layered intrusion (southwest Norway): a jotunite (hypersthene monzodiorite)-derived A-type granitoid suite. *Journal of Petrology* **38**, 337–369.
- Eby, G. N. (1985). Monteregian Hills II. Petrography, major and trace element geochemistry and strontium isotopic chemistry of the eastern intrusions: Mounts Shefford, Brome, and Megantic. *Journal of Petrology* **26**, 418–448.
- Emslie, R. F. (1985). Proterozoic anorthosite massifs. *NATO ASI Series C: Mathematical and Physical Sciences* **158**, 39–60.
- Ewart, A., Oversby, V. M. & Mategan, A. (1977). Petrology and isotope geochemistry of Tertiary lavas from the northern flank of the Tweed volcano, Southeastern Queensland. *Journal of Petrology* **18**, 73–113.
- Ferguson, J. (1970). The differentiation of agpaitic magmas; the Ilimaussaq intrusion, south Greenland. *Canadian Mineralogist* **10**, 335–359.
- Frost, B. R. & Lindsley, D. H. (1992). Equilibria among Fe–Ti oxides, pyroxenes, olivine, and quartz: Part II. Application. *American Mineralogist* **77**, 1004–1020.
- Frost, B. R., Arculus, R. J., Barnes, C. G., Collins, W. J., Ellis, D. J. & Frost, C. D. (2001). A geochemical classification of granitic rocks. *Journal of Petrology* **42**, 2033–2048.
- Frost, B. R., Frost, C. D., Cornia, M., Chamberlain, K. R. & Kirkwood, R. (2006). The Tetón–Wind River domain: a 2.68–2.67 Ga active margin in the western Wyoming Province. *Canadian Journal of Earth Sciences* **43**, 1489–1510.

- Frost, C. D. & Frost, B. R. (1997). High-K, iron-enriched rapakivi-type granites: the tholeiite connection. *Geology* **25**, 647–650.
- Frost, C. D. & O'Nions, R. K. (1985). Caledonian magma genesis and crustal recycling. *Journal of Petrology* **26**, 515–544.
- Frost, C. D., Frost, B. R., Chamberlain, K. R. & Edwards, B. R. (1999). Petrogenesis of the 1.43 Ga Sherman batholith, SE Wyoming: a reduced rapakivi-type anorogenic granite. *Journal of Petrology* **40**, 1771–1802.
- Haapala, I., Rämö, O. T. & Frindt, S. (2005). Comparison of Proterozoic and Phanerozoic rift-related basaltic–granitic magmatism. *Lithos* **80**, 1–32.
- Hanan, B. B., Shervais, J. W. & Vetter, S. K. (2008). Yellowstone plume–continental lithosphere interaction beneath the Snake River Plain. *Geology* **36**, 51–54.
- Henderson, C. M. B., Pendlebury, K. & Foland, K. A. (1989). Mineralogy and petrology of the Red Hill alkaline igneous complex, New Hampshire, USA. *Journal of Petrology* **30**, 627–666.
- Hildreth, W., Halliday, A. N. & Christiansen, R. L. (1991). Isotopic and chemical evidence concerning the genesis and contamination of basaltic and rhyolitic magma beneath the Yellowstone plateau volcanic field. *Journal of Petrology* **32**, 63–138.
- Jacobson, R. R. E., MacLeod, W. N. & Black, R. (eds) (1958). *Ring-complexes in the Younger Granite Province of Northern Nigeria*. Geological Society, London, *Memoirs* **1**, 72 pp.
- King, P. L., Chappell, B. W., Allen, C. M. & White, A. J. R. (2001). Are A-type granites the high-temperature felsic granites? Evidence from fractionated granites of the Wangrah Suite. *Australian Journal of Earth Sciences* **38**, 501–514.
- Krishna Reddy, K., Ratnakar, J. & Leelanandam, C. (1998). A petrochemical study of the Proterozoic alkaline complex of Uppalapadu, Prakasam Province, Andhra Pradesh, India. *Journal of the Geological Society of India* **52**, 41–52.
- Kumar, V. K., Frost, C. D., Frost, B. R. & Chamberlain, K. R. (2007). The origin of the Chimakurti–Uppalapadu plutons, Eastern Ghats belt, India: An unusual association of tholeiitic, A-type and alkaline magmatism. *Lithos* **97**, 30–57.
- LaFort, P. (1980). Manaslu leucogranite: a collision signature of the Himalaya, a model for its genesis and emplacement. *Journal of Geophysical Research* **86**, 10545–10568.
- Larsen, E. S. (1948). *Batholith and Associated Rocks of Corona, Elsinore and San Luis Rey Quadrangles Southern California*. Geological Society of America, *Memoirs* **29**, 182 pp.
- Leeman, W. P., Smith, D. R., Hildreth, W., Palacz, S. & Rogers, N. (1990). Compositional diversity of Late Cenozoic basalts in a transect across the southern Washington Cascades: Implications for subduction zone magmatism. *Journal of Geophysical Research* **95**, 19561–19582.
- Le Maitre, R. W. (ed.) (1989). *A Classification of Igneous Rocks and Glossary of Terms*. Oxford: Blackwell Scientific, 193 pp.
- Le Roex, A. P., Cliff, R. A. & Adair, B. J. I. (1990). Tristan da Cunha, South Atlantic: Geochemistry and petrogenesis of basanite–phonolite lava series. *Journal of Petrology* **31**, 799–812.
- Loiselle, M. C. & Wones, D. R. (1979). Characteristics and origin of anorogenic granites. *Geological Society of America, Abstracts with Programs* **11**, 468.
- Longhi, J. & Ashwal, L. D. (1985). Two-stage models for lunar and terrestrial anorthosites: petrogenesis without a magma ocean. *Journal of Geophysical Research* **90**, C571–C584.
- Longhi, J., Fram, M. S., Vander Auwera, J. & Montieth, J. N. (1993). Pressure effects, kinetics, and rheology of anorthositic and related magmas. *American Mineralogist* **78**, 1016–1030.
- MacDonald, G. A. (1968). Composition and origin of Hawaiian lavas. In: Coats, R. R., Hay, R. L. & Anderson, C. A. (eds) *Studies in Volcanology. A memoir in honor of Howell Williams*. Geological Society of America *Memoir* **116**, 477–522.
- Malm, O. A. & Ormaasen, D. E. (1978). Mangerite–charnockite intrusives in the Lofoten–Vesterålen Area, North Norway: Petrography, chemistry, and petrology. *Norges Geologiske Undersøkelse* **338**, 83–114.
- Marsh, B. D. & Carmichael, I. S. E. (1974). Benioff zone magmatism. *Journal of Geophysical Research* **79**, 1196–1206.
- McBirney, A. R. & Williams, H. (1969). *Geology and Petrology of the Galapagos Islands*. Geological Society of America, *Memoirs* **118**, 197 pp.
- Melson, W. G., Vallier, T. L., Wright, T. L., Byerly, G. & Nelen, J. (1976). Chemical diversity of abyssal volcanic glass erupted along Pacific, Atlantic and Indian Ocean sea-floor spreading centers. In: Sutton, G. H., Manghnani, M. H. & Moberly, R. (eds) *The geophysics of the Pacific Ocean basin and its margin. A volume in honor of George P. Woodland*. *Geophysical Monograph* **19**. Washington, DC: American Geophysical Union, pp. 351–367.
- Mirnejad, H. & Bell, K. (2006). Origin and source evolution of the Leucite Hills lamproites: Evidence from Sr–Nd–Pb–O isotopic compositions. *Journal of Petrology* **47**, 2463–2489.
- Miyashiro, A. (1974). Volcanic rocks series in island arcs and active continental margins. *American Journal of Science* **274**, 321–355.
- Morse, S. A. (1980). Kiglapait mineralogy. II. Fe–Ti oxide minerals and the activities of oxygen and silica. *Journal of Petrology* **21**, 685–719.
- Nash, W. P. & Wilkinson, J. F. G. (1970). Shonkin Sag Laccolith, Montana. I. Mafic minerals and estimates of temperature, pressure, oxygen fugacity and silica activity. *Contributions to Mineralogy and Petrology* **25**, 241–269.
- Nash, W. P. & Wilkinson, J. F. G. (1971). Shonkin Sag Laccolith, Montana. II. Bulk rock geochemistry. *Contributions to Mineralogy and Petrology* **33**, 162–170.
- Nash, W. P., Carmichael, I. S. E. & Johnson, B. W. (1969). The mineralogy and petrology of Mount Suswa, Kenya. *Journal of Petrology* **10**, 409–439.
- Nicol, A. & Wallace, L. M. (2007). Temporal stability of deformation rates: comparison of geologic and geodetic observations, Hikurangi subduction margin, New Zealand. *Earth and Planetary Science Letters* **258**, 397–413.
- Orajaka, I. P. (1986). geochemistry of Kaffo valley albite–riebeckite–granite, Liruei granite ring-complex, northern Nigeria. *Chemical Geology* **56**, 85–92.
- Osborn, E. F. (1959). Role of oxygen pressure in the crystallization and differentiation of basaltic magma. *American Journal of Science* **257**, 609–647.
- Parsons, I. (1981). The Klokken gabbro–syenite complex, South Greenland: Quantitative interpretation of mineral chemistry. *Journal of Petrology* **22**, 233–260.
- Patiño Douce, A. E. & Beard, J. A. (1995). Dehydration-melting of biotite gneiss and quartz amphibolite from 3 to 15 kbar. *Journal of Petrology* **36**, 707–738.
- Patiño Douce, A. E. & Beard, J. A. (1996). Effects of $P, f(\text{O}_2)$ and Mg/Fe ratio on dehydration melting of model metagreywackes. *Journal of Petrology* **37**, 999–1024.
- Peacock, M. A. (1934). Classification of igneous rock series. *Journal of Geology* **39**, 689–710.
- Rapp, R. P., Watson, E. B. & Miller, C. F. (1991). Partial melting of amphibolite/eclogite and the origin of Archean trondhjemitic and tonalites. *Precambrian Research* **51**, 1–25.

- Riishuus, M. S., Peate, D. W., Tegner, C., Wilson, J. R. & Brooks, C. K. (2008). Petrogenesis of cogenetic silica-oversaturated and -undersaturated syenites by periodic recharge in a crustally contaminated magma chamber: the Kangerlussuaq Intrusion, East Greenland. *Journal of Petrology* **49**, 493–522.
- Schoenenberger, J., Marks, M., Wagner, T. & Markl, G. (2006). Fluid–rock interaction in autoliths of agpaitic nepheline syenites in the Ilimaussaq intrusion, South Greenland. *Lithos* **91**, 331–351.
- Scoates, J. S. (2000). The plagioclase–magma density paradox re-examined and the crystallization of Proterozoic anorthosites. *Journal of Petrology* **41**, 627–649.
- Scoates, J. S., Frost, C. D., Mitchell, J. N., Lindsley, D. H. & Frost, B. R. (1996). A residual liquid origin for monzonitic rocks in Proterozoic anorthosite complexes: The Sybille intrusion, Laramie Anorthosite Complex, Wyoming. *Geological Society of American Bulletin* **108**, 1357–1371.
- Shand, S. J. (1922). The problem of the alkaline rocks. *Proceedings of the Geological Society of South Africa* **25**, xix–xxxiii.
- Shand, S. J. (1947). *The Eruptive Rocks*, 3rd edn. New York: John Wiley, 444 pp.
- Smithies, R. H., Champion, D. C. & Cassady, K. F. (2003). Formation of Earth's early Archean continental crust. *Precambrian Research* **127**, 89–101.
- Sørensen, H. (1960). On the agpaitic rocks. *International Geologic Congress. Report of the Twenty-First Session Norden* **13**, 319–327.
- Stoltz, A. J. (1985). The role of fractional crystallization in the evolution of the Nandewar Volcano, north-eastern New South Wales, Australia. *Journal of Petrology* **26**, 1002–1026.
- Sutton, A. N., Blake, S., Wilson, C. J. N. & Charlier, B. L. A. (2000). Late Quaternary evolution of a hyperactive rhyolite magmatic system, Taupo Volcanic Center, New Zealand. *Journal of the Geological Society, London* **157**, 537–557.
- Ussing, N. V. (1912). Geology of the country around Julianehaab, Greenland. *Meddelelser om Grønland* **38**, 1–426.
- Valiquette, G. & Archambault, G. (1970). Les gabbros et les syenites du complexe de Brome. *Canadian Mineralogist* **10**, 48–510.
- Vernon, R. H. (1986). K-feldspar megacrysts in granites—phenocrysts, not porphyroblasts. *Earth-Science Reviews* **23**, 1–63.
- Weiss, S. & Troll, G. (1989). The Ballachulish Igneous Complex, Scotland: Petrography, mineral chemistry and order of crystallization in the monzodiorite–quartz diorite suite and in the granite. *Journal of Petrology* **30**, 1069–1115.
- Whitaker, M. L., Nekvasil, H., Lindsley, D. H. & McCurry, M. (2008). Can crystallization of olivine tholeiite give rise to potassic rhyolites?—an experimental investigation. *Bulletin of Volcanology* **70**, 417–434.
- Zen, E. (1988). Phase relations of peraluminous granitic rocks and their petrogenetic implications. *Annual Review of Earth and Planetary Sciences* **16**, 21–52.